Inorganic Chemistry

Article

pubs.acs.org/IC

Molecular Dyads of Ruthenium(II)− or Osmium(II)−Bis(terpyridine) Chromophores and Expanded Pyridinium Acceptors: Equilibration between MLCT and Charge-Separated Excited States

Jérôme Fortage,[†,‡] Grégory Dupeyre,[†] Fabien Tuyèras,[†] Valérie Marvaud,[‡] Philippe Ochsenbein,[§] Ilaria Ciofini,[∥] Magdaléna Hromadová,[⊥] Lubomír Pospísil,[⊥] Antonino Arrigo,[#] Emanuela Trovato,[#] Fausto Puntoriero,*[,#] Philippe P. Lainé,*[,†] and Sebastiano Campagna*[,#]

[†]Univ Paris Diderot, Sorbonne Paris Cité, ITODYS, UMR CNRS 7086, 15 rue J-A de Baïf, 75013 Paris, France

[‡]UPMC, Université Paris 06, Institut Parisien de Chimie Moléculaire, UMR 7201 CNRS, Case 42, 4 place Jussieu, 75005 Paris, France

[§]Laboratoire de Cristallographie et Modélisation Moléculaire du Solide, Sanofi LG-CR, 371 rue du Professeur Blayac, 34184 Montpellier CEDEX 04, France

[∥]École Nationale Supérieure de Chimie de Paris − Chimie ParisTech, LECIME, UMR 7575 CNRS, 11 rue Pierre et Marie Curie, 75005 Paris, France

[⊥]J. Heyrovský Institute of Physical Chemistry of ASCR, v.v.i., Dolejškova 3, 18223 Prague, Czech Republic

[#]Dipartimento di Scienze Chimiche, Università di Messina, and Centro Interuniversitario per la Conversione Chimica dell'Energia Solare (SOLARCHEM), Via F. Stagno d'Alcontres 31, I-98166 Messina, Italy

Supporting Information

ABSTRACT: The synthesis, characterization, redox behavior, and photophysical properties (both at room temperature in fluid solution and at 77 K in rigid matrix) of a series of four new molecular dyads (**2**−**5**) containing Ru(II)− or Os(II)−bis(terpyridine) subunits as chromophores and various expanded pyridinium subunits as electron acceptors are reported, along with the reference properties of a formerly reported dyad, **1**. The molecular dyads **2**−**4** have been designed to have their (potentially emissive) triplet metal-to-ligand charge-transfer (MLCT) and charge-separated (CS) states close in energy, so that excited-state equilibration between these levels can take place. Such a situation is not shared by limit cases **1** and **5**. For dyad **1**, forward photoinduced electron transfer (time constant, 7 ps) and subsequent charge recombination (time constant, 45 ps) are evidenced, while for dyad **5**, photoinduced electron transfer is thermodynamically forbidden so that MLCT decays are the only active deactivation processes. As regards **2**−**4**, CS states are formed from MLCT states with time constants of a few dozens of picoseconds. However, for these latter species, such experimental time constants are not due to photoinduced charge separation but are related to the excited-state equilibration times. Comparative analysis of time constants for charge recombination from the CS states based on proper thermodynamic and kinetic models highlighted that, in spite of their apparently affiliated structures, dyads **1**−**4** do not constitute a homologous series of compounds as far as intercomponent electron transfer processes are concerned.

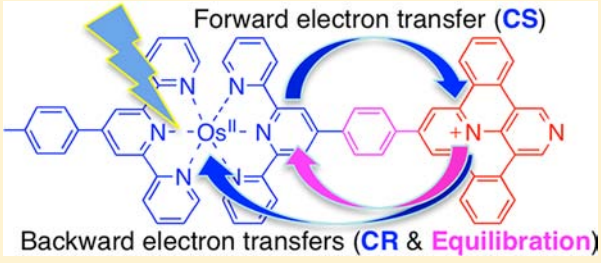

INTRODUCTION

Photoinduced electron transfer (ET) continues to be at the center of growing interest for fundamental and applicative reasons.[1,2] The enormous amount of studies devoted to purposedly conceived two-component systems (i.e., molecular dyads) has allowed the disentanglement and investigation of the various effects that intramolecular electronic coupling, nuclear reorganization (including solvent dynamics), and ET driving forces have on both the efficiency and the rate constants of charge separation and charge recombination processes. However, relatively little investigation has involved molecular dyads exhibiting a driving force for charge separation close to zero.[3−5]

Recently, we investigated the photophysical properties of molecular dyads (D−S−A) made of Ru(II)− or Os(II)−bis(tpy) complexes (with tpy = 2,2′:6′,2″-terpyridine) functioning as photosensitizing chromophores and primary electron donors (D), on the one hand, and of expanded (bi)pyridinium subunits serving as electron acceptors (A), on the other hand, variously connected by oligophenylene-type linear bridges as

Received: June 27, 2013
Published: October 3, 2013

Chart 1. Structural Formulae of the Studied Molecular Dyads 1−5 and of Their Model Species[a]

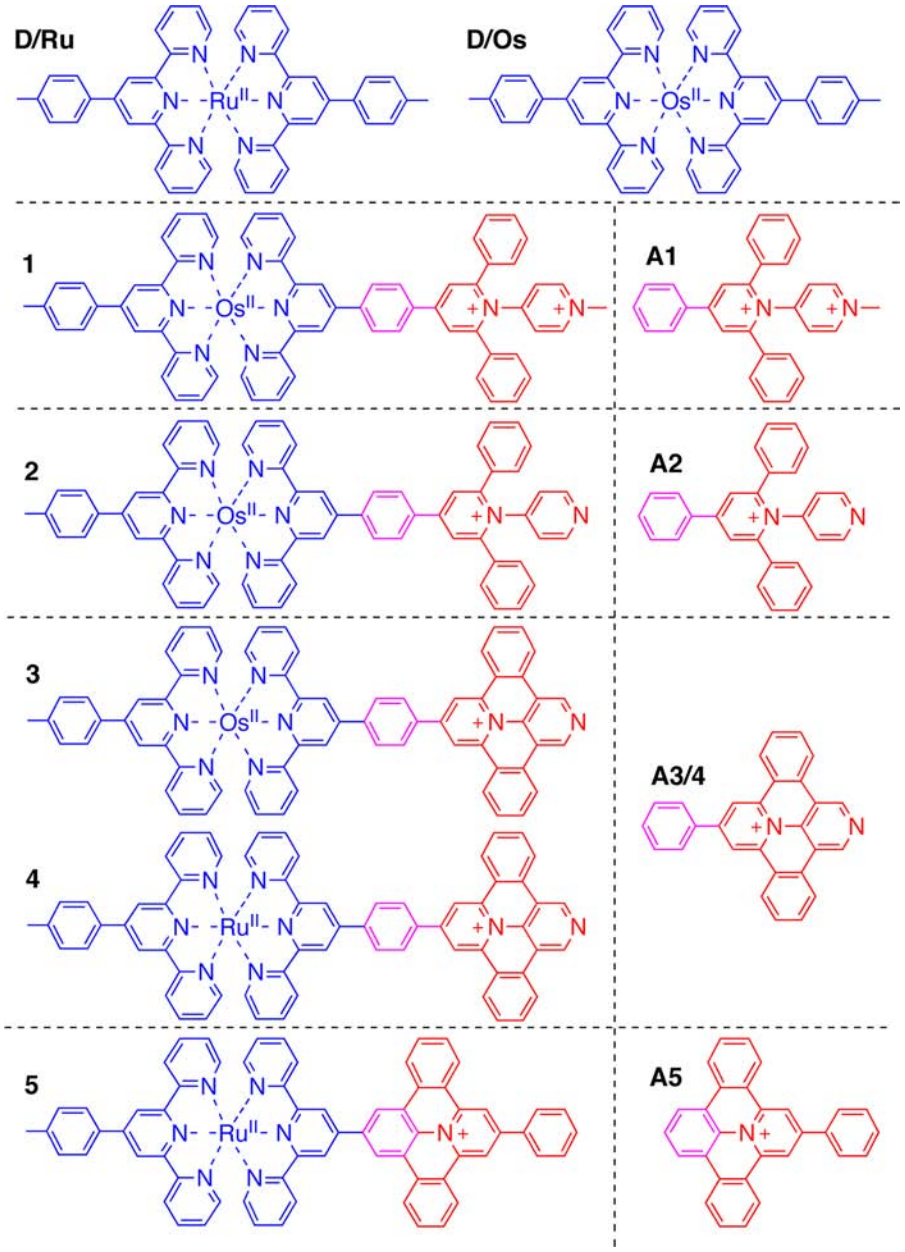

[a]Note that **A3/4** is the acceptor reference model for both **3** and **4**.

spacers (S).[6] In the course of that study, we suggested that replacing biphenylene bridges with monophenylene spacers is a strategy likely to favor the formation (and accumulation) of charge-separated (CS) states. Indeed, the less pronounced electron-donating character of the latter spacers allows circumventing of the bridge-assisted mechanism of charge recombination, when the photoinduced process leading to the preparation of such CS states is an oxidative electron transfer. In a further step of design of molecular dyads, we report here on the synthesis, characterization, redox behavior, and photophysical properties of a series of four new compounds of the same family (**2**−**5**; Chart 1), plus one compound (dyad **1**; Chart 1) whose properties have been partially reported in a previous paper,[6] all of them containing a single phenylene moiety as the spacer. As regards the driving force for photoinduced electron transfer between the initially prepared metal-to-ligand charge-transfer (MLCT) excited state of the metal-based chromophore (D) and the expanded pyridinium acceptor (A) to produce the targeted $[D^+-S-A^-]$ CS state, its value is close to zero for most of the dyads here studied. This peculiar situation allows us to investigate the effect of a possible excited-state equilibration between MLCT and CS states on the photophysical properties of the studied compounds.

The molecular structures of the series of dyads under consideration are shown in Chart 1, together with the structures of reference species, namely model bis(4′-tolyl-tpy) metal complexes (**D**/**M**, with M = Ru and Os) as reference photosensitizers and electrophoric expanded pyridiniums (EPs) as reference acceptor species (**A***n*, with *n* = 1−5).

dx.doi.org/10.1021/ic401639g | *Inorg. Chem.* 2013, 52, 11944−11955

RESULTS AND DISCUSSION

Synthetic Strategy. With regard to the kind of semirigid photosensitizer−(spacer)−acceptor dyads investigated here, the control of intramolecular charge separation goes through concomitantly achieving two types of development, which are the aforementioned engineering of the spacer,[6,7] and the fine-tuning of ET driving forces. The latter parameter largely relies on the chemical variability of the acceptor component.[8] The study of several series of model acceptors of 1,2,4,6-tetra-substituted-pyridinium type, **TP** (i.e., $[R^0Ar\text{-}\mathbf{TP}R^1{}_2R^2]^+$, Figure 1a), showed the importance of their *N*-aryl group (R^0Ar) whose nature can be changed to make their first reduction potential fall in the proper range (typically $E_{1/2}{}^{red} \geq -0.6$ V vs SCE) to produce efficient intramolecular ET. In this respect, a choice group is pyridyl (py) that becomes an efficient electron-withdrawing substituent when quaternized (R^0−Ar is methyl-pyridylium, Me-py).[7,9−11] The same tuning method holds for the *fused* polycyclic derivatives of these tetraarylpyridinium molecules, ***f*TP** (Figure 1a), reaching similarly good reduction behavior to that of the benchmark electron acceptor methyl viologen **MV** (i.e., $E_{1/2}{}^{red} \approx -0.4$ V vs SCE) in the case of the fused counterpart of dicationic species $[\text{Me-py-}\mathbf{TP}R^1{}_2R^2]^{2+}$ (with $R^1 = R^2 = H$; Figure 1a).[9] From a synthetic viewpoint, exploitation of the appealing acceptor properties of these new bis-N-heterocyclic acceptors for charge separation requires inversion of the topology of the dyads as compared to that of dyads of the first generation.[5,12] This is achieved by moving the inorganic photosensitizer (D component) from the R^0 position of the pyridinium-based A component to its R^2 position (Figure 1b). Insofar as the scope of the present study deals with ET driving forces approaching zero, only dyads made up of *monocationic* **TP** (i.e., **A2**) and ***f*TP** (**A3**/**4** and **A5**) types of EPs are investigated, the two-component D−(S)−A system built from *dicationic* **A1** serving as a reference[6] (Chart 1).

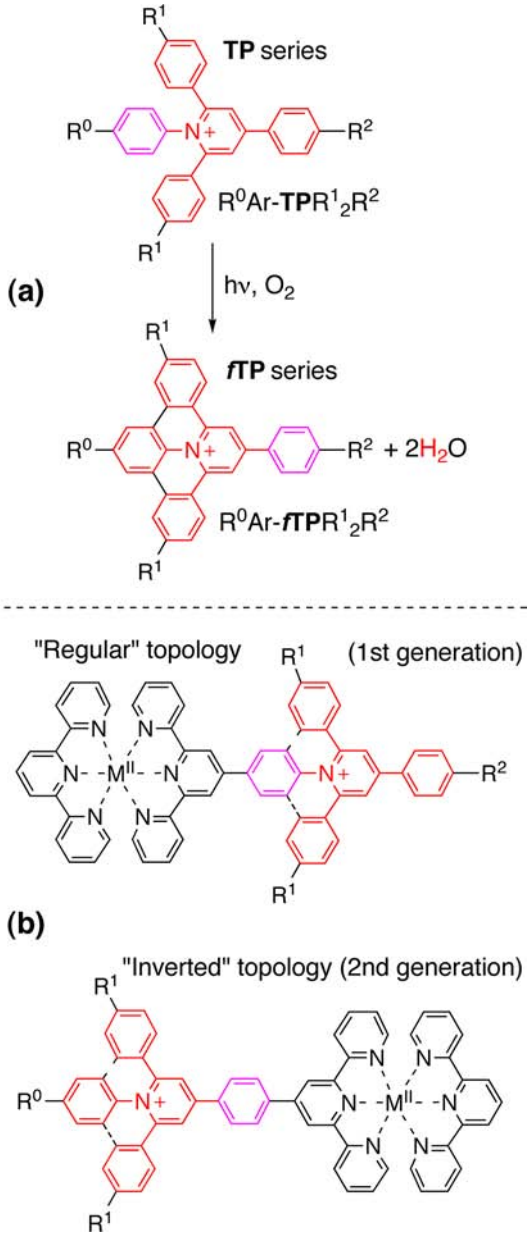

Figure 1. (a) Molecular structures of the two types of expanded pyridiniums (**TP** and ***f*TP**) serving as electron acceptors (A) in D−(S)−A dyads. (b) Connection schemes corresponding to D−(S)−A dyads of the first ("regular" topology; D @ R^0) and second ("inverted" topology; D @ R^2) generations; M = Ru, Os.

Another aspect that deserves comment deals with the photochemistry of EPs of the branched **TP** type and their possible transformation into ***f*TP** derivatives (Figure 1a).[9,10,13] Some branched EPs are intrinsically stable vis-à-vis photobiscyclization, as is the case for **A1**,[7,9] and those potentially light-sensitive, like **A2**, are actually protected from photo-induced pericondensation by the presence of the covalently linked inorganic photosensitizer (D) when embedded within dyads (case of **2**).[5,12] Indeed, within these D−(S)−A assemblies, ultrafast funneling of electronic energy (excitation) occurs toward the D-centered lowest excited state (^{3}MLCT) that works as an energy sink (likely *via* the ^{1}MLCT state), thereby inhibiting the EP-centered photochemistry (that normally takes place in the UV domain). From the synthetic viewpoint, it follows that ligands bearing a *fused* EP must be prepared before carrying out coordination chemistry (i.e., strategy based on "photochemistry on the complex" with dyads built from branched EPs of **TP** type is not operative). Thus, ligand tpy-**A3**/**4** (giving dyads **3** and **4**) was prepared by coupling the boronic ester of the chelating tpy fragment with the suitable bromo-derivative of **A3**/**4**, and ligand tpy-**A5** (giving dyad **5**) was obtained photochemically from the tpy-ph-$\mathbf{TP}H_3^+$ precursor. All details are given in the Supporting Information. Structural features typical of dyads built from ***f*TP** acceptors are revealed by single-crystal X-ray crystallography in the representative case of rod-like dyad **5** (see Figure 2). Observed curvature of the molecular backbone of **5** is not due to crystal packing but originates from some intrinsic structural constraints of the fused EP, as evidenced by previous theoretical[11] and experimental (X-ray crystallography)[14] studies.

Redox Behavior. All the studied compounds undergo a reversible one-electron oxidation and several reversible reduction processes, which are in some cases bielectronic in nature (see below and Figures S15−S19 in Supporting Information). As usual for Ru(II)− and Os(II)−polypyridine complexes,[15] the single-electron oxidation is ascribed to a metal-centered process, and the reduction processes are assumed to be ligand-centered. As the relevant redox processes for photoinduced electron transfer and charge separation are the first reduction and oxidation processes, only related values of potential are reported in Table 1 for all the studied dyads,

dx.doi.org/10.1021/ic401639g | Inorg. Chem. 2013, 52, 11944−11955

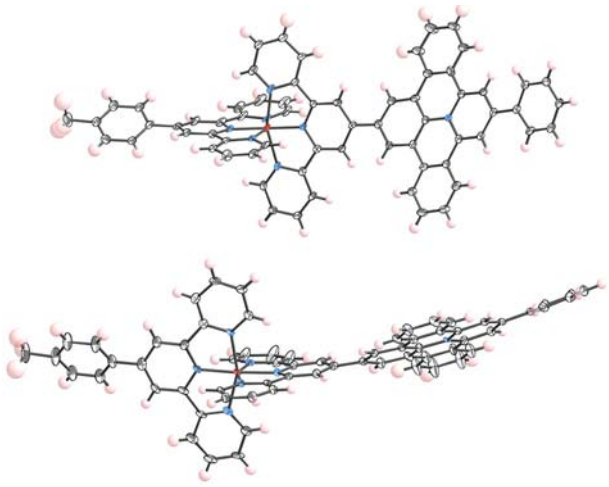

Figure 2. Orthogonal views of $[(ttpy)Ru(tpy\text{-}\mathbf{A5})]^{3+}$ complex (**5**) with thermal ellipsoids (50% probability), showing the topology of first generation dyads (ttpy is 4′-tolyl-tpy).

Table 1. Relevant Redox Data of the Studied Dyads and of Their Model Species (vs SCE) at Pt Electrode for Acetonitrile Solution (0.1 M NBu_4PF_6) at Room Temperature[a,b]

compound	$E_{1/2}^{ox}$, V (ΔE_p, mV)	$E_{1/2}^{red}$, V (ΔE_p, mV)
1	+0.91 (59)	−0.53[c] (59)
A1		*−0.60*[c] *(102)*[d]
2	+0.91 (69)	−0.86[c] (69)
A2		*−0.93*[c] *(115)*[d]
3	+0.90 (80)	−0.76 (80)
A3/4		*−0.84 (114)*[d]
4	+1.24 (90)	−0.70 (90)
5	+1.26 (80)	−0.90 (80)
A5		*−1.00 (117)*[d]
D/Os	+0.88 (68)	−1.22 (68)
D/Ru	+1.22 (80)	−1.27 (80)

[a] $E_{1/2}$ (vs SCE) is calculated as $(E_{pa} + E_{pc})/2$, where E_{pa} and E_{pc} are the anodic and cathodic peak potentials measured by cyclic voltammetry at 0.1 V s^{-1}; ΔE_p is the difference of potential between E_{pc} and E_{pa}. [b] The data referring to the isolated acceptors are shown in italics. [c] Two-electron process (see ref 17). [d] From ref 9.

together with the corresponding redox potentials of **D/M** and ***An*** model species. From comparison with the **TP** and ***f*TP** pyridinium-based references (**A1**, **A2**, **A3/4**, and **A5**), the first reduction processes observed for dyads **1**−**5** are straightforwardly assigned to their respective expanded (bi)pyridinium subunits, as expected. Moreover, the close similarity observed between redox potentials recorded for dyad systems and related model components allows for inferring that electronic interaction between metal-based (D) and pyridinium (A) subunits in **1**−**5** is relatively weak, so these species can actually be considered as multicomponent, supramolecular species,[16] at least from a redox viewpoint.

Finally, it is worth noting that the first reduction process in **1** and **2** is of a bielectronic nature. Indeed, it has been demonstrated that the corresponding **A1** and **A2** branched EPs undergo a two-electron reduction as a result of a redox potential *compression/inversion* that originates in a large structural rearrangement, namely pyramidalization of the $N_{pyridinio}$ atom of their pyridinium core, upon reduction.[17] Here, it is important to stress that for such a type of electrochemical behavior, the potential for the one-electron first reduction coincides with that of the experimentally recorded bielectronic process.[17,18] So, the reduction potentials reported, although experimentally related to a bielectronic process, are suitable to calculate thermodynamic parameters for photoinduced electron transfer processes (inherently one-electron processes) to the expanded pyridinium subunit(s), when Koopmans' theorem is assumed as valid.

Absorption Spectra. Absorption spectra of **1**−**5** are dominated by metal-to-ligand charge-transfer (MLCT) bands in the visible region and by slightly metal-perturbed ligand-centered (LC) bands in the UV, as expected for Ru(II) and Os(II) polypyridine complexes.[15,19] Figure 3 shows the spectra

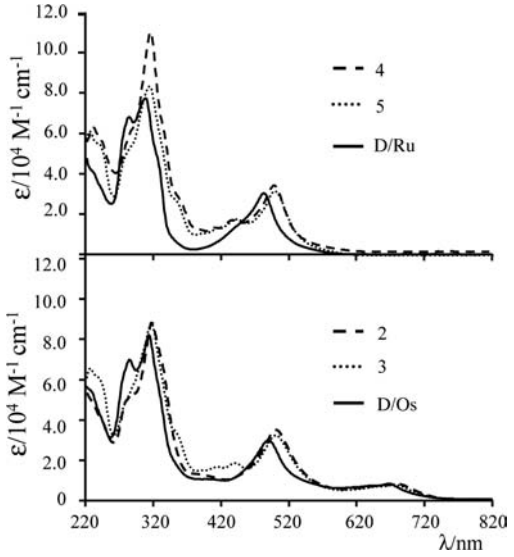

Figure 3. Absorption spectra of some of the studied compounds in acetonitrile solution and comparison with their model complexes. The compounds reported are indicated within the panels.

of some selected compounds, whereas data of all the chromophoric assemblies are collected in Table 2. Spectra of osmium compounds **1**−**3** display both ^{1}MLCT and ^{3}MLCT bands, while only the spin-allowed ^{1}MLCT bands are shown by the ruthenium species **4** and **5**. MLCT bands of molecular dyads are slightly red-shifted in comparison with those of **D/Ru** and **D/Os** model compounds (Table 2), suggesting non-negligible electronic interaction between the metal-based chromophoric unit (D) and the acceptor pyridinium subsystems (A) at the ground state. Acceptor subunits contribute to the near-UV−vis region absorption, in particular in dyads based on the fused acceptors **A3/4** and **A5** (that is, **3**−**5**). Structured absorption features are indeed observed in the 360−450 nm range (Figure 3) that are due to the vibronic contribution of the lowest-energy spin-allowed $\pi-\pi^*$ transitions centered on the ***f*TP** acceptor subunit(s).[9−11,20] For **1** and **2**, where the nonfused (i.e., branched) **A1** and **A2** pyridinium moieties are present, the lowest-energy $\pi-\pi^*$ transitions occur at higher energy,[9] so the corresponding absorption bands are overlapped with other (phenyl-tpy) LC bands.

Photophysical Properties. Compounds **2**−**5** exhibit luminescence both at room temperature in fluid acetonitrile solution and at 77 K in a butyronitrile rigid matrix, whereas **1** emits only at 77 K (Table 2). In all cases, emission can be

Table 2. Absorption and Luminescence Data[a]

species	absorption[b] λ_{max}, nm (ε, 10^4 M^{-1} cm^{-1})		luminescence, 298 K			luminescence, 77 K	
	^{1} MLCT	^{3} MLCT	λ_{max}, nm	τ, ns	ϕ	λ_{max}, nm	τ, μs
1	499 (3.4)	673 (0.9)		no emission		733	2.7
2	498 (3.6)	673 (1.0)	760	2.1	4.0×10^{-4}	730	2.8
3	499 (3.2)	673 (0.9)	760	1.1	1.6×10^{-5}	733	2.7
4	497 (3.7)		685	15	1.4×10^{-4}	663	15.0
5	499 (3.5)		670	8	2.4×10^{-4}	640	12.1
D/Os	495 (3.0)	668 (0.8)	740	240	2.0×10^{-2}	720	2.9
D/Ru	492 (3.0)		647	1	3.2×10^{-5}	628	12.5

[a]Absorption and 298 K emission data were recorded from air-equilibrated acetonitrile solutions. Emission data at 77 K were collected from butyronitrile rigid glasses. [b]Only the lowest energy MLCT absorption band maxima are reported.

assigned to ^{3}MLCT states.[15,19,21,22] For osmium-based dyads, the emission spectra are only slightly displaced to the red compared with those of the model species **D/Os**, both in fluid solution and at 77 K, whereas the red shift is larger for the emission spectra of ruthenium-containing dyads compared to those of the model species **D/Ru**. At 77 K, the luminescence lifetimes of all the compounds are in the 2−3 μs range for the osmium species and in the 10−15 μs range for the ruthenium ones, in accordance with energy gap law. Moreover, emission lifetimes of all the molecular dyads are close to those of the corresponding model species, indicating that no further excited-state decay process is present, at 77 K, with respect to the decay processes already present in the models. On the contrary, emission lifetimes and quantum yields of **2** and **3** are largely reduced compared to **D/Os** at room temperature in fluid solution (as mentioned above, room temperature emission is totally absent for **1**). Conversely, under the same experimental conditions, emission lifetimes and quantum yields of the ruthenium-containing dyads are larger than those of **D/Ru**. All the luminescence data are collected in Table 2, and the luminescence spectra of some representative compounds are shown in Figure 4.

Although small, the bathochromic shift of the emission spectra of **1**−**3** osmium compounds compared to that of **D/Os** suggests that the presence of the expanded pyridinium subunits perturbs the MLCT state of the inorganic chromophore. Such a perturbation can be ascribed to the electron-withdrawing effect

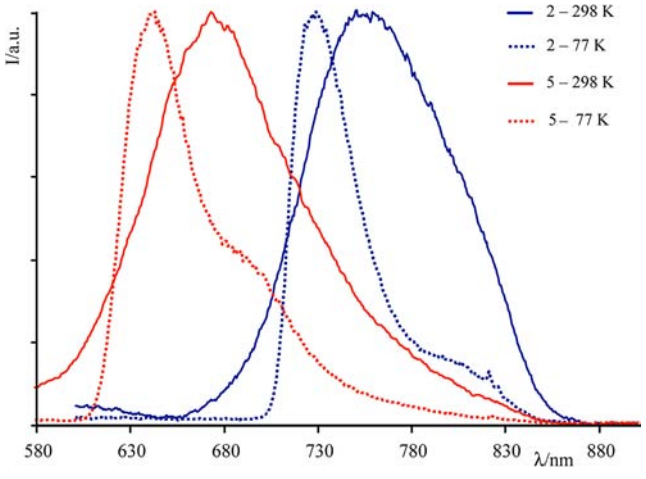

Figure 4. Luminescence spectra (uncorrected for PMT response) of **2** (blue lines) and **5** (red lines). Solid lines refer to emission spectra in acetonitrile at room temperature, and dotted lines refer to emission spectra in butyronitrile at 77 K.

that the positive charge, carried by the pyridinium acceptor, exerts on the chelating tpy fragment, with the ultimate result of slightly decreasing the MLCT state energy.

In principle, in multicomponent species like **1**−**5**, photoinduced electron transfer from the D-centered excited MLCT state to the pyridinium subunits, playing the role of oxidative electron transfer quenchers, can occur, thereby yielding a charge separated state, CS (see Figure 5 for a pictorial

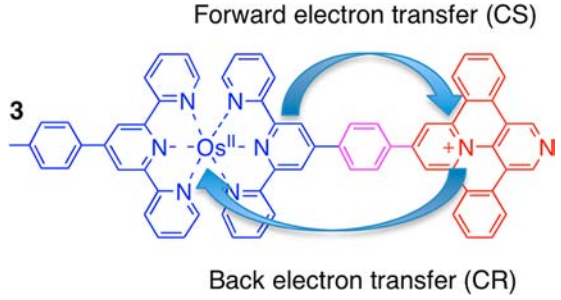

Figure 5. Pictorial representation of the charge separation process (indicated as electron transfer) and charge recombination (back electron transfer) in a representative compound, **3**. The charge separation process could be regarded as a charge shift within the "tpy-pyridinium" segmented ligand, as it corresponds to an electron density shift from a terpyridine-based orbital toward a pyridinium-based one, with the two subunits directly connected via the phenylene spacer.

representation of the process; note that the photoinduced electron transfer process could be alternatively regarded as a shift of electron density within the "tpy-pyridinium" segmented ligand).[23] This was indeed demonstrated to occur in **1**.[6]

The driving force for photoinduced electron transfer, ΔG^0_{ET}, can be approximated by eq 1.[15]

$$\Delta G^0_{ET} = (*E_{ox} - E_{red}) + W \quad (1)$$

$$*E_{ox} = E_{ox} - E^{00} \quad (2)$$

In eq 1, $*E_{ox}$ is the oxidation potential of the excited state of the chromophoric (primary) electron donor (expressed, as all the other similar terms in eqs 1 and 2, as one-electron energies, in eV), in its turn approximated from eq 2, where E_{ox} is the ground-state oxidation potential of the donor and E^{00} is the (MLCT) excited-state energy, approximated to the highest-energy maximum of the emission spectrum at 77 K.[15] The term E_{red} is the reduction potential of the acceptor. The term W, called the work term, is the difference between Coulombic stabilization energies of reactants and products; its effect, which

dx.doi.org/10.1021/ic401639g | Inorg. Chem. 2013, 52, 11944−11955

is to (slightly) reduce the driving force, is however often neglected.

From the data in Tables 1 and 2, ΔG^0_{ET} values for photoinduced electron transfer in **1**−**5** are calculated and shown in Table 3. The obtained values indicate that such an

Table 3. Driving Forces and Time Constants for Forward Electron Transfer (ET) and Charge Recombination (CR) in 1−4 in Acetonitrile at Room Temperature[a]

compound	$(k)_{ET}^{-1}$, ps	$\Delta G_{ET}{}^0$, eV[b]	$(k)_{CR}^{-1}$, ps	$\Delta G_{CR}{}^0$, eV[c]
1	7	−0.25	45	−1.44
2	28[d]	+0.12	2095[e] (41)[f]	−1.81
3	20[d]	−0.03	950[g] (575)[f]	−1.66
4	35[d]	+0.08	15000[e]	−1.94

[a]Compound **5** is not reported here since its driving force for charge separation (+0.22 eV, from eq 1) makes the process definitely forbidden. [b]Calculated by eq 1. [c]From eq 3. [d]This figure refers to MLCT and CS equilibration processes (see text). [e]From luminescence data. It is not the time constant for charge recombination but the lifetime of the equilibrated state. [f]Estimated time constant for charge recombination, according to eq 5 (see text). [g]Lifetime of the equilibrated state, from transient spectra decay. It is in good agreement with the observed luminescence lifetime (1.1 ns, see Table 2). The value derived from the transient data (950 ps) is preferred for successive calculations of charge recombination rate constants.

excited-state decay process is (moderately) exergonic for **1** and thermodynamically forbidden for **5**, whereas for compounds **2**−**4** the MLCT and CS states, that is the reactant and product of the formal intramolecular photoinduced electron transfer, are roughly iso-energetic. The modest (at the best) values of ΔG^0 for photoinduced electron transfer calculated for all the series of compounds justify the 77 K emission properties of **1**−**5**, as even in the case of **1**, having the more favorable thermodynamics at room temperature in fluid solution, the destabilization of the charge-separated states and/or the presence of nuclear barriers, well-known at 77 K in rigid matrix,[24,25] make electron transfer inefficient under these conditions.

To investigate photoinduced electron transfer processes, pump−probe transient absorption spectroscopy is quite useful. Dyad **1** can be taken as a model species for photoinduced electron transfer in this series of compounds. Indeed, as already reported,[6] upon light excitation at 400 nm the initial transient spectrum (i. e., the transient spectrum recorded after 400 fs from laser pulse), typical of Os-terpyridine ^{3}MLCT states, evolves to that attributed to a charge-separated product. Indication for the CS state is a growing transient absorption in the 500−550 nm range, characteristic of reduced expanded (bi)pyridinium,[6] which is concomitant with the decay of the transient absorption due to the reduced terpyridine moiety (550−700 nm).[12b,26] The new transient spectrum directly decays to the ground state (charge recombination). In a former report,[6] rate constants for charge separation and charge recombination occurring in **1** were based on global fitting of the data and were calculated to be about 12 and 35 ps, respectively. Now, we repeated the experiments and found that more precise values are 7 (±3) ps and 45 (±8) ps, respectively, slightly correcting the former values. For comparison, the initial transient absorption spectrum of **D**/**Os**, practically identical to the initial transient spectrum of **1** except for the (expected) small shift of the MLCT absorption bleaching, directly decays to the ground state without any relevant spectral change.[6]

The time-resolved transient spectra of **2**−**4** are shown in Figures 6−8. For all of them, besides the prominent bleach near

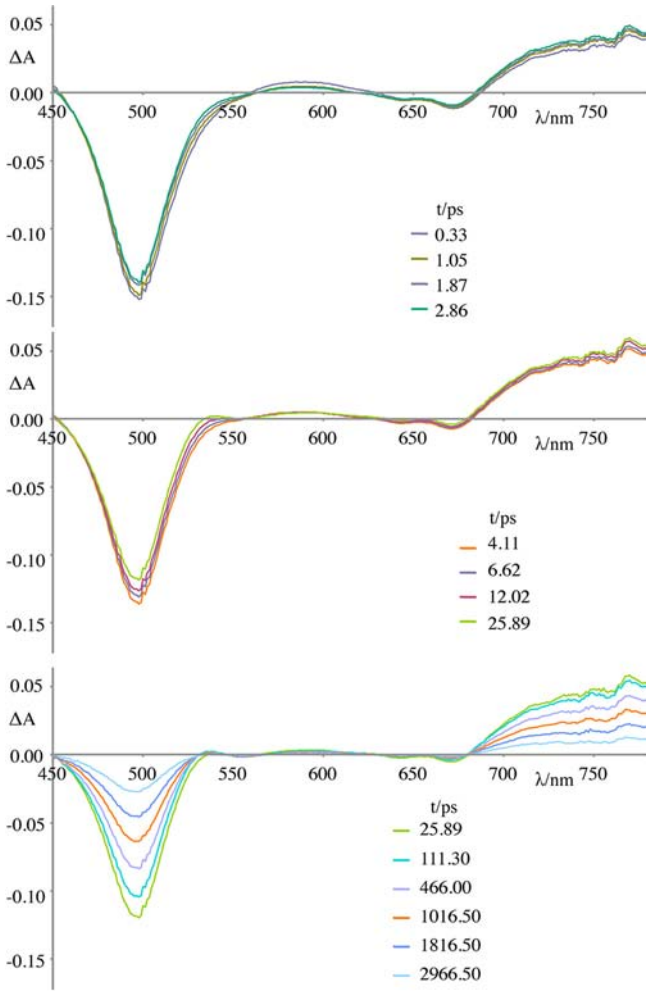

Figure 6. Transient absorption spectra (TAS) of Os-based dyad **2** in acetonitrile (λ_{pump} = 400 nm). Top panel: TAS registered in the first 3 ps after the pump pulse (note a first process with small changes in absorption in the 550−650 nm spectral range). Middle panel: TAS registered in the time range 4−26 ps (note the increase of transient absorption in the 500−550 nm range simultaneous with a further decrease of the absorption in the 550−650 nm range). Bottom panel: TAS registered in the time range 26−3000 ps corresponding to the decay to the ground state.

500 nm, attributed to the bleaching of the spin-allowed MLCT absorption, a first process involving changes in the transient absorption region due to reduced terpyridine (in the 550−650 nm spectral range and at wavelengths longer than 700 nm) is observed, with a time constant of about 2−3 ps.[27] A very similar process was also exhibited by **1**.[6] This process, already reported for ruthenium and osmium complexes with polypyridine-type ligands carrying a phenyl substituent,[12c,28] includes ultrafast planarization of the phenylene ring bridging the inorganic chromophore and the expanded pyridinium acceptor. However, an internal conversion from the (higher-energy) MLCT state involving the peripheral tolyl-terpyridine to the (lower-energy) MLCT state involving the terpyridine linked via the phenylene spacer to the acceptor unit, cannot be excluded. Successively, spectral changes that are qualitatively similar to one another occur for species **2**−**4**. In summary, such spectral changes

dx.doi.org/10.1021/ic401639g | Inorg. Chem. 2013, 52, 11944−11955

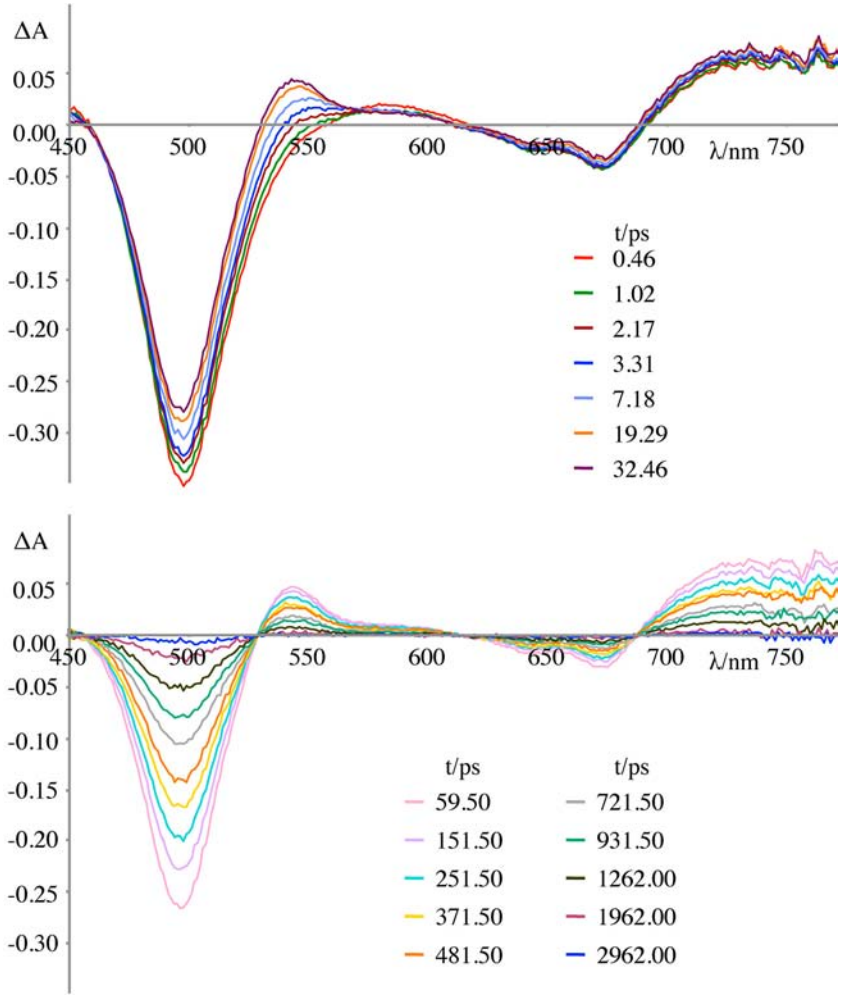

Figure 7. Transient absorption spectra (TAS) of Os-based dyad **3** in acetonitrile (λ_{pump} = 400 nm). Top panel: TAS registered in the first 35 ps after the pump pulse (note the increase of transient absorption in the 500−550 nm range simultaneous with the decrease of the absorption in the 550−650 nm range). Bottom panel: TAS registered in the time range 60−3000 ps corresponding to the recovery of the ground state. A quite broad transient absorption is present at wavelengths longer than 700 nm for all the compounds here studied. The discussion of the transient spectra in more detail than reported in the main text is quite difficult due to many possible transitions typical of the excited state.

consist of the increase of transient absorption in the 500−550 nm range, with a concomitant decrease of the absorption related to the reduced terpyridine-based fragment in the 550−700 nm range (see Figure 6, middle panel, and Figures 7 and 8, top panels). Similar spectral changes are again qualitatively similar to those already reported for **1**, for which they were attributed to the formation of the CS state.[6] This suggests that CS states are formed from the initially prepared MLCT states also in **2**−**4**. Rate constants for such processes are reported in Table 3. Afterward, the so-formed transient spectra decay to the ground state (Figures 6−8, bottom panels). For **2** and **3**, the transient spectra decay to the ground state within about 2 and 1 ns, respectively. In the case of **4**, such a decay is extremely slow, so that it cannot be fitted within 3.2 ns, which is the upper time limit of our ultrafast equipment.

As regards **5**, photoinduced electron transfer cannot take place since the process is definitely endoergonic (+0.22 eV, according to eq 1). In fact, its transient absorption spectra do not exhibit the time evolution shown by those of **1**−**4**, leading to population of the CS state, but the relaxed MLCT state, once formed, directly decays to the ground state on a time scale that is longer than 3.2 ns (Figure 9), according to luminescence lifetime data (i.e., 8 ns; Table 2).

At first glance, it is tempting to assign the decays of the final transient spectra of **2**−**4** to charge recombination (CR), i.e. to the direct decays of the charge-separated states to the ground states. Incidentally, under this assumption, calculating the approximate driving force for recombination, ΔG^0_{CR}, from eq 3 (with E^{00} and $\Delta G_{ET}{}^0$ having the meanings reported above, and also using the rate constants for the formation of the CS state as the electron transfer rate constants) and plotting ln k against ΔG^0 would surprisingly suggest that the forward and backward electron transfer processes of all the complexes could lie on the same Marcus-type curve (see Figure S20 in Supporting Information). However, such a conclusion, which would imply identical reorganization energies for the forward and back electron transfer schematized in Figure 5, is clearly wrong.

$$\Delta G^0_{CR} = E^{00} + \Delta G^0_{ET} \quad (3)$$

In fact, whereas the kinetic data for **1** refer to genuine charge separation and recombination processes, this is not the case for **2**−**4**, as also suggested by their incompletely quenched (Os) or even enhanced (Ru) D-centered emission as compared to reference **D**/**Os** and **D**/**Ru** respective models (Table 2). Energies of MLCT and CS states for such dyads are so close

dx.doi.org/10.1021/ic401639g | *Inorg. Chem.* 2013, 52, 11944−11955

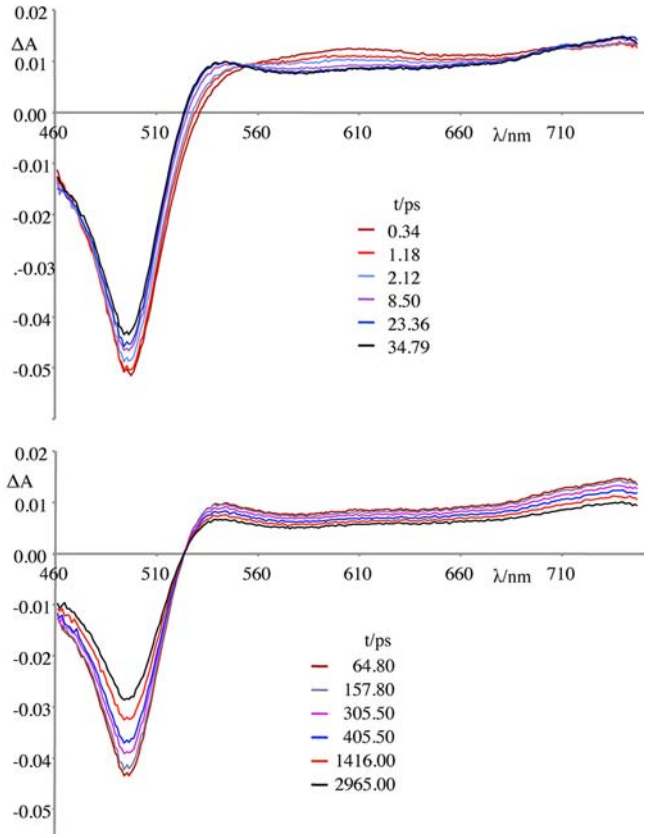

Figure 8. Transient absorption spectra (TAS) of Ru-based dyad **4** in acetonitrile (λ_{pump}= 400 nm). Top panel: TAS registered in the first 35 ps after the pump pulse (note the increase of transient absorption in the 500−550 nm range simultaneous with the decrease of the absorption in the 550−700 nm spectral range). Bottom panel: TAS registered in the time range 60−3000 ps corresponding to the initial recovery of the ground state.

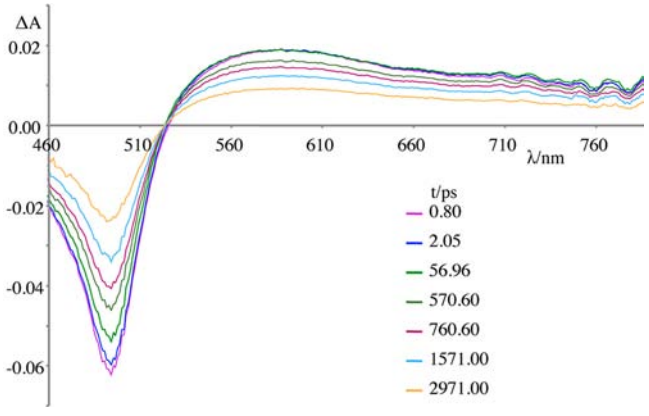

Figure 9. Transient absorption spectra (TAS) of Ru-based dyad **5** in acetonitrile (λ_{pump}= 400 nm), registered in the time range 0.8 ps to 3 ns after the pump pulse.

that thermal equilibration between the two states is feasible and even quite probable. This requires that the back electron transfer from the CS state to the MLCT state is faster than charge recombination to the ground state, an expected behavior because of thermodynamic and electronic considerations.[29] The features of the room-temperature emission exhibited by **2**−**4** (see Table 2) definitely indicate that the ^{3}MLCT state is still present even after the excited state decay leading to the CS state has taken place (see ultrafast transient absorption data). This can be rationalized assuming that the process occurring in the 20−40 ps range in **2**−**4** is indeed an equilibration process, leading to a mixture of CS and ^{3}MLCT states. In this case, the observed rate constants for the apparent formation of the CS states are the summation of forward and backward electron transfers, not the rate constants for the photoinduced electron transfer (forward) process.[30] The situation is reminiscent of excited-state equilibration between closely lying ^{3}MLCT states and triplet $\pi-\pi^*$ levels of organic chromophores in some multichromophoric systems based on polypyridine metal complexes and fused aromatic hydrocarbons, capable of leading to delayed and long-lived MLCT emission.[31] The fact that the measured k_{ET} values of dyads **2**−**4** are roughly constant (see Table 3), in spite of changes in driving force for charge separation, further supports the equilibrium hypothesis. In fact, the experimental rate constant is the sum of forward and reverse rate constants, and the expected changes in the two rate constants in **2**−**4** will probably tend to cancel out in the sum.

With the reasonable assumption that direct decays from MLCT and CS states to the ground state are negligible with respect to excited-state equilibrium rate constants, the relative percentages of MLCT and CS states at the equilibrium can be obtained from the usual Boltzmann distribution, as in eq 4.

$$\alpha = \exp(-\Delta G/k_B T) \tag{4}$$

In eq 4, α is the percentage of the higher energy state[32] (with $(1-\alpha)$ the percentage of the lower-lying state), ΔG is the energy difference between the two states (in this specific case, assumed to be equivalent to ΔG^0_{ET}), k_B is the Boltzmann constant, and T is the temperature. Because of the small values of $\Delta G_{ET}{}^0$ calculated for **2**−**4**, and the approximations used (first of all, the experimental uncertainty in redox potentials (10 mV) and the approximation of W to zero), α absolute values calculated by eq 4 should be considered with care. However, eventual errors should be largely constant in the series, so the results are expected to be qualitatively valid when internally compared.

By using eq 4, the percentage of CS state at the equilibrium increases on going from **2** and **4** (for both compounds, it is calculated to be less than 10%) to **3**, for which it is calculated to be about 60%. Apart from the effective percentages, and also considering the differences between **A2** and **A3**/**4** (that are the pyridinium subunits present in **2** and in **3** and **4**), so that corresponding reduced species may show slightly different absorption spectra (e.g., see Supporting Information Figures S21−S22 for the spectroelectrochemistry of **A2** and **A3**/**4**), the comparison between the transient absorption spectra of **2**−**4** after the occurrence of the equilibration process (Figures 6−8) indicates that the peak at about 540 nm, characteristic of the CS state, is more prominent in **3**, thus confirming that the equilibrated excited state of this latter species has a larger percentage of CS state compared to molecular dyads **2** and **4**.

According to the excited-state equilibration hypothesis, the experimental rate constants for the processes leading to the ground state for compounds **2**−**4** are not charge recombination rate constants but refer to the overall decay of the equilibrated state. In a first approximation, the charge recombination rate constants from the CS states to the ground state can still be calculated, by using eq 5.

$$k_{exp} = \mathrm{MLCT}_{percentage} \times k_{MLCT} + \mathrm{CS}_{percentage} \times k_{CR} \tag{5}$$

dx.doi.org/10.1021/ic401639g | Inorg. Chem. 2013, 52, 11944−11955

In eq 5, k_{exp} is the experimental rate constant of the overall equilibrated state, which is obtained from transient data for **2** and **3** and from luminescence data for **4**. MLCT and CS percentages are the same percentages as those calculated by eq 4 (see above). k_{MLCT} is the reciprocal of the emission lifetime of the corresponding model species (i.e, the intrinsic decay of the MLCT state, in the absence of the pyridinium unit). Actually, this calculation can be attempted only for the osmium species, for which the perturbation of the acceptor subunits on the MLCT state is relatively small (see above), so that **D**/**Os** can be considered a sufficiently good model to which to refer. It is not applicable to **4**, since the emission data suggest that the **D**/**Ru** model has MLCT excited-state energy and therefore decay dynamics, much too different from that of **4** (see Table 2; in particular, 77 K emission data are quite informative on this issue). So, the rate constant of the intrinsic decay processes of the MLCT state of **D**/**Ru** cannot be used as a model for the k_{MLCT} value of **4**.

From eq 5, time constants for charge recombination from the CS state to the ground state are 41 and 575 ps for **2** and **3**, respectively (Table 3; note that the α value in eq 4 is not related to the same state in the series of compounds;[32] this should be carefully considered when performing calculations). When the time constant for charge recombination in **1** is also considered (45 ps) and the k_{CR}'s of the series are compared to the driving force ΔG_{CR}^{0} values (Table 3), it appears that no obvious relationship exists between driving force and rate constant for the process. This finding indicates that compounds **1**−**3** are not members of a homologous series as regards intercomponent electron transfer processes, thereby testifying that the pyridinium-based acceptor subunits in **1**−**3**(**4**) are different from one another as far as both the localization of the LUMO (the acceptor orbital of the CS state) and nuclear reorganization connected to electron transfer processes are concerned. Indeed, LUMO is essentially localized on the pendant pyridylium *N*-group for the dicationic acceptor component of **1**, whereas it is located on the pyridinium core in the other dyads.[9−11,17] As regards redox-induced rearrangements, they essentially relate back to the *branched* (**TP** type in **1** and **2**) and *fused* (***f*TP** type in **3** and **4**) natures of acceptor subsystems.

A final comment is warranted as far as the luminescence properties of the ruthenium species here studied are concerned. For both **4** and **5**, emission lifetimes at room temperature are longer (and quantum yields are larger) than that of their model species **D**/**Ru** (Table 2). This is in line with the MLCT decay of Ru-terpyridine compounds.[15,19] In fact, in these species, the main pathway for excited state decay is the thermally activated radiationless decay that involves an upper-lying metal-centered (MC) level close in energy. In such a type of compound, decreasing the energy of the MLCT state (following the impact of the electron-withdrawing effect exerted by the weakly interacting A component) has the effect of increasing the energy barrier between MLCT and MC levels (on assuming that the energy of the MC level remains unchanged, as expected for the present compounds), so that the efficiency of the thermally activated process is ultimately decreased and the luminescence properties are improved.[15,33]

CONCLUSION

A series of molecular dyads **2**−**5** built from Os(II)−or Ru(II)−bis-terpyridine subunits as photosensitizers (D) and expanded pyridinium units as electron acceptors (A) has been prepared, and its absorption spectra, redox behavior, and photophysical properties have been studied, together with corresponding features of the already reported compound **1**, here included as a reference compound for charge separation. The spectroscopic and redox data indicate that the chromophoric (D) and electron accepting (A) subunits are only weakly interacting in the ground state, the intercomponent electronic interaction being however larger for the Ru(II) compounds than for the Os(II) species.

Whereas for **5** the ^{3}MLCT state is the lowest-energy level of the whole compound (so once formed, it directly decays to the ground state), in the multicomponent systems **2**−**4** the energy of the ^{3}MLCT state is close to the energy of the charge-separated (CS) state obtained by photoinduced electron transfer from the ^{3}MLCT level to the expanded pyridinium unit (Figure 10). This allowed us to investigate the effect of

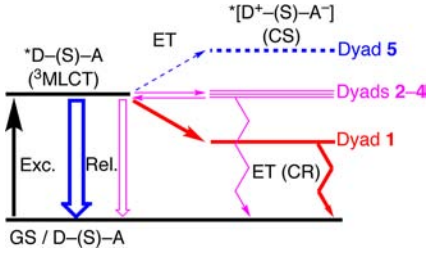

Figure 10. Energy level diagram: pictorial representation of various cases (GS = ground state, Exc. = excitation, Rel. = relaxation and ET = electron transfer). For details, see main text.

excited-state equilibration between MLCT and CS states on the room temperature photophysical properties of the compounds. In particular, **2**−**4** exhibit MLCT emission, whose lifetimes and quantum yields depend on the equilibration ratio between the equilibrated states. This definitely indicates that the presence of CS states, even when the photoinduced electron transfer is (moderately) endoergonic, cannot be neglected to interpret the luminescence properties of multicomponent compounds.

The presence of the CS state is evidenced in **2**−**4** by transient absorption spectroscopy, via formation of the reduced pyridinium subunit(s) as chromophoric probes in the 520−560 nm region, with time constants of a few dozens of picoseconds. However, such experimental time constants are not due to photoinduced charge separation but are related to the excited-state equilibration times. The time constants for charge recombination from the CS states for **2** and **3** can be estimated by thermodynamic and kinetic model data, and when the related data for **1** are also considered, it is clear that, in spite of the apparent similitude in structures, the molecular dyads investigated here do not represent a homologous series as far as intercomponent electron transfer processes are concerned.

Overall, the present study provides further insight into the manner by which intramolecular photoinduced electron transfers can occur within multicomponent systems in spite of driving forces virtually approaching zero. Moreover, this work also demonstrates the methodological relevance of the detailed investigation of series of compounds that undergo such phenomena and share closely affiliated features at both structural and electronic levels when it is a matter of identifying and disentangling the subtle factors that will serve for subsequent design of functional assemblies intended to finely manage processes as sensitive as photoinduced electron transfers. In particular, within the framework of artificial

dx.doi.org/10.1021/ic401639g | *Inorg. Chem.* 2013, 52, 11944−11955

photosynthesis, one can envision conceiving new photochemical molecular devices that rely on charge-separation processes with such very low driving forces to minimize energy loss during some energy transduction steps.

EXPERIMENTAL SECTION

Syntheses, Characterization, and General Experimental Details. Materials, syntheses of organic ligands and related inorganic dyads, along with full characterizations are provided in the Supporting Information.

Crystal Structure Determination. Highly instable tiny plate crystals could be hardly grown from an acetonitrile/diethyl ether mixture. Intensity data were collected at a low temperature (113 K) on a Bruker APEX-II diffractometer (IμS, Cu Kα, λ = 1.54178 Å, graphite monochromator) in ω and ϕ scan modes, with sample-to-detector distances of 50 mm. The data were corrected for Lorentz, polarization, and absorption effects. The structure was solved by direct methods with SIR2011[34] and refined by full-matrix least-squares based on F^2 using SHELXTL.[35] CCDC-942738 contains the supplementary crystallographic data for this paper. These data can be obtained free of charge from The Cambridge Crystallographic Data Centre via www.ccdc.cam.ac.uk/data_request/cif

Crystal Data for [5](PF$_6$)$_3$. $(C_{66}H_{44}N_7Ru)\cdot 3(PF_6)\cdot(CH_3CN)\cdot 1.25(C_2H_5OC_2H_5)\cdot 1.25(H_2O)$, M = 3266.0, monoclinic, $P2/c$ (No. 13), a = 20.2820(9), b = 8.4250(4), c = 40.1465(18)Å, α = 90.000, β = 91.210(3), γ = 90.000°; V = 6858.5(5), Z = 2, ρ_{calc} = 1.568 g cm^{-3}, μ = 3.435 mm^{-1}, $F(000)$ = 3261.0, 68 301 observed reflections ($2\theta_{max}$ = 134.7°, R_{int} = 0.098). The asymmetric unit contains one tricationic complex, three hexafluorophosphate anions distributed over four sites—all but one being disordered or having partial occupancy—one acetonitrile, two disordered diethyl ether, and two half-water molecules. Anisotropic least-squares refinements were carried out for all non-hydrogen atoms. Hydrogens were included in calculated positions according to a riding model; no hydrogen atom was defined for solvent molecules. Similarity (σ = 0.04), planarity (σ = 0.1), and bond distance (σ = 0.05) restraints were applied to all species. Refinements: $R[F^2 > 2\sigma(F^2)]$ = 0.099, R (all data) = 0.123, wR2 (all data) = 0.229, S = 2.09 for 10 406 data, 4555 restraints, and 1110 parameters. Final difference Fourier synthesis shows two maxima (3.5 and 3.1 e/Å^3) close (1.07 and 1.08 Å) to the position of the Ru atom, similarly to the crystal structure of previously reported cationic bis-terpyridyl ruthenium(II) complexes.[5b,12a] This feature may indicate that the crystal contains a minor twin component, as also suggested by about a hundred reflections having observed intensities strongly larger than the calculated one. The next maxima of residual electronic densities stand in the expected range (<0.7 eÅ^{-3}).

Electrochemical Measurements. Electrochemical experiments were carried out with a conventional three-electrode cell and a PC-controlled potentiostat/galvanostat (Princeton Applied Research Inc. model 263A). The working electrode was a platinum electrode from Radiometer-Tacussel (area, 0.0314 cm^2; diameter, 2.0 mm) mounted in Teflon. Platinum wire was used as the counter-electrode and a saturated calomel electrode (SCE) as the reference. Electrolytic solutions, MeCN (Aldrich, anhydrous, 99.8%) containing 0.1 M tetrabutylammonium hexafluorophosphate (TBAPF$_6$, Aldrich, +99%) as a supporting electrolyte, were routinely deoxygenated by argon bubbling. All potential values are given versus the SCE. The reported numerical values (Table 1) were corrected by using a dissolved Fc$^+$/Fc couple as an internal reference and by setting $E_{1/2}$ (Fc$^+$/Fc) equal to +0.380 V vs SCE in MeCN.[36] Cyclic voltammetry experiments were conducted at a scan rate of 0.1 V s^{-1}. Experimental uncertainty on potential values is 10 mV.

UV–Vis–NIR Spectroelectrochemistry. UV–vis–NIR spectroelectrochemical measurements were obtained with the optically transparent thin-layer electrode (OTTLE) cell of the construction described previously.[17] The inlet and outlet openings allowed filling the cell with degassed samples under anaerobic conditions. Cyclic voltammograms were obtained concurrently with the UV–vis–NIR spectra using a potentiostat/galvanostat EG&G 263 (Princeton Applied Research, U.S.A.) at scan rates of 20 mV s^{-1}, while the spectra were sampled every 2 s using a diode-array UV–vis–NIR spectrometer (Agilent, model 8453). TBAPF$_6$ (+99%), supporting electrolyte, and acetonitrile solvent (anhydrous, 99.8%) were supplied by Sigma-Aldrich and dried before use.

Absorption Spectra and Photophysical Properties. UV–vis absorption spectra were taken on a Jasco V-560 spectrophotometer. For steady-state luminescence measurements, a Jobin Yvon-Spex Fluoromax 2 spectrofluorimeter was used, equipped with a Hamamatsu R3896 photomultiplier. The spectra were corrected for photomultiplier response using a program purchased with the fluorimeter. For the luminescence lifetimes, an Edinburgh OB 900 time-correlated single-photon-counting spectrometer was used. As excitation sources, a Hamamatsu PLP 2 laser diode (59 ps pulse width at 408 nm) and/or the nitrogen discharge (pulse width 2 ns at 337 nm) were employed. For luminescence quantum yield, the optically dilute method was employed,[37] using $[Ru(bpy)_3]^{2+}$ in air-equilibrated aqueous solution as a quantum yield standard (Φ = 0.028).[38] Time-resolved transient absorption experiments were performed by using a pump–probe setup based on the Spectra-Physics MAI-TAI Ti:sapphire system as the laser source and the Ultrafast Systems Helios spectrometer as the detector. The pump pulse was generated with a Spectra-Physics 800 FP OPA. The probe pulse was obtained by continuum generation on a sapphire plate (spectral range, 450–800 nm). The effective time resolution was ca. 200 fs. The temporal chirp over the white-light in the 450–750 nm range was ca. 150 fs. The temporal window of the optical delay stage was 0–3200 ps. The time-resolved data were analyzed with the Ultrafast Systems Surface Explorer Pro software. Experimental uncertainties on the absorption and photophysical data are as follows: absorption maxima, 2 nm; molar absorption, 15%; luminescence maxima, 4 nm; luminescence lifetimes, 10%; luminescence quantum yields, 20%; transient absorption decay and rise rates, 10%.

ASSOCIATED CONTENT

Supporting Information

Experimental details for the synthesis and characterization of new compounds and precursors including ^{1}H NMR (500 MHz) and ^{13}C NMR (126 MHz) spectra as well as ESI mass spectra; cyclic voltammograms of dyads **1**–**5**; apparent Marcus relationship; UV–vis spectroelectrochemical study (reduction regime) of model acceptors **A2** and **A3**/**4**. X-ray crystallographic data for [**5**](PF$_6$)$_3$ in CIF format. This material is available free of charge via the Internet at http://pubs.acs.org.

AUTHOR INFORMATION

Corresponding Authors

*E-mail: campagna@unime.it.
*E-mail: philippe.laine@univ-paris-diderot.fr.
*E-mail: fpuntoriero@unime.it.

Notes

The authors declare no competing financial interest.

ACKNOWLEDGMENTS

The authors are thankful to Dr. F. Bedioui and Dr. S. Griveau for fruitful discussions. A.A., E.T., F.P., and S.C. thank MIUR (FIRB Nanosolar and PRIN projects) and PON-Energetics for financial support. G.D., F.T., V.M., and P.P.L. are grateful to the French National Agency for Research (ANR) "programme blanc" (SWITCH project: ANR-2010-BLAN-712) for financial support. M.H. and L.P. greatly acknowledge the financial support from the Academy of Sciences of the Czech Republic (M200401202).

REFERENCES

(1) The literature on this topic is too vast to be exhaustively quoted. For some examples, see: (a) Closs, G. L.; Miller, J. D. *Science* **1988**, *240*, 440. (b) Meyer, T. J. *Acc. Chem. Res.* **1989**, *22*, 163. (c) Newton, M. D. *Chem. Rev.* **1991**, *91*, 767. (d) Wasielewski, M. R. *Chem. Rev.* **1992**, *92*, 435. (e) Onuchic, J. J.; Beratan, D. N.; Winkler, J. R.; Gray, H. B. *Annu. Rev. Biophys. Biomol. Struct.* **1992**, *21*, 349. (f) Gust, D.; Moore, T. A.; Moore, A. L. *Acc. Chem. Res.* **1993**, *26*, 198. (g) Paddon-Row, M. N. *Acc. Chem. Res.* **1994**, *27*, 18. (h) Barbara, P. F.; Meyer, T. J.; Ratner, M. A. *J. Phys. Chem.* **1996**, *100*, 13148. (i) Verhoeven, J. W. *Adv. Chem. Phys.* **1999**, *106*, 603. (j) Gust, D.; Moore, A. L.; Moore, T. A. *Acc. Chem. Res.* **2001**, *34*, 40. (k) Baranoff, E.; Collin, J.-P.; Flamigni, L.; Sauvage, J.-P. *Chem. Soc. Rev.* **2004**, *33*, 147. (l) Benniston, A. C.; Harriman, A. *Chem. Soc. Rev.* **2006**, *35*, 169. (m) Wasielewski, M. R. *J. Org. Chem.* **2006**, *71*, 5051.

(2) (a) *Electron Transfer in Chemistry*; Balzani, V., Ed.; Wiley-VCH: Weinheim, Germany, 2001; Vols. *1*−*5*. (b) Fukuzumi, S. *Bull. Chem. Soc. Jpn.* **2006**, *79*, 177. (c) Rodriguez-Morgade, M. S.; Torres, T.; Atienza-Castellanos, C.; Guldi, D. M. *J. Am. Chem. Soc.* **2006**, *12*, 15145. (d) Albinsson, B.; Martersson, J. *J. Photochem. Photobiol. C: Photochem. Rev.* **2008**, *9*, 138. (e) Colvin, M. T.; Butler Ricks, A.; Wasielewski, M. R. *J. Phys. Chem. A* **2012**, *116*, 2184.

(3) (a) Heitele, H.; Finckh, P.; Weeren, S.; Pöllinger, F.; Michel-Beyerle, M. E. *J. Phys. Chem.* **1989**, *93*, 5173. (b) Kuciauskas, D.; Liddell, P. A.; Lin, S.; Stone, S. G.; Moore, A. L.; Moore, T. A.; Gust, D. *J. Phys. Chem. B* **2000**, *104*, 4307. (c) Yamazaki, M.; Araki, Y.; Fujitsuka, M.; Ito, O. *J. Phys. Chem. A* **2001**, *105*, 8615. (d) Cotlet, M.; Masuo, S.; Luo, G.; Hofkens, J.; Van der Auweraer, M.; Verhoeven, J.; Müllen, K.; Xie, X. S.; De Schryver, F. *Proc. Natl. Acad. Sci. U. S. A.* **2004**, *101*, 14343. (e) Kawauchi, H.; Suzuki, S.; Kozaki, M.; Okada, K.; Islam, D.-M. S.; Araki, Y.; Ito, O.; Yamanaka, K. *J. Phys. Chem. A* **2008**, *112*, 5878. (f) Ren, G.; Schlenker, C. W.; Ahmed, E.; Subramaniyan, S.; Olthor, S.; Kahn, A.; Ginger, D. S.; Jenekhe, S. A. *Adv. Funct. Mater.* **2013**, *23*, 1238.

(4) (a) Borgström, M.; Johansson, O.; Lomoth, R.; Berglund Baudin, H.; Wallin, S.; Sun, L.; Åkermark, B.; Hammarström, L. *Inorg. Chem.* **2003**, *42*, 5173. (b) Hanss, D.; Wenger, O. S. *Eur. J. Inorg. Chem.* **2009**, 3778.

(5) (a) Lainé, P.; Amouyal, E. *Chem. Commun.* **1999**, 935. (b) Lainé, P.; Bedioui, F.; Ochsenbein, P.; Marvaud, V.; Bonin, M.; Amouyal, E. *J. Am. Chem. Soc.* **2002**, *124*, 1364. (c) Ciofini, I.; Lainé, P. P.; Bedioui, F.; Adamo, C. *J. Am. Chem. Soc.* **2004**, *126*, 10763.

(6) Fortage, J.; Puntoriero, F.; Tuyèras, F.; Dupeyre, G.; Arrigo, A.; Ciofini, I.; Lainé, P. P.; Campagna, S. *Inorg. Chem.* **2012**, *51*, 5342.

(7) Fortage, J.; Tuyèras, F.; Peltier, C.; Dupeyre, G.; Calboréan, A.; Bedioui, F.; Ochsenbein, P.; Puntoriero, F.; Campagna, S.; Ciofini, I.; Lainé, P. P. *J. Phys. Chem. A* **2012**, *116*, 7880.

(8) Obviously, ET driving force can also be tuned via the choice of the metal ion (e.g., Ru(II), Os(II)) of the coordination complex that plays the role of the D component. This is illustrated by the couple of dyads **3** and **4** (Chart 1), as shown later (see Table 3 in the following).

(9) Fortage, J.; Peltier, C.; Nastasi, F.; Puntoriero, F.; Tuyèras, F.; Griveau, S.; Bedioui, F.; Adamo, C.; Ciofini, I.; Campagna, S.; Lainé, P. P. *J. Am. Chem. Soc.* **2010**, *132*, 16700.

(10) Fortage, J.; Tuyèras, F.; Ochsenbein, P.; Puntoriero, F.; Nastasi, F.; Campagna, S.; Griveau, S.; Bedioui, F.; Ciofini, I.; Lainé, P. P. *Chem.—Eur. J.* **2010**, *16*, 11047.

(11) Peltier, C.; Adamo, C.; Lainé, P. P.; Campagna, S.; Puntoriero, F.; Ciofini, I. *J. Phys. Chem. A* **2010**, *114*, 8434.

(12) (a) Lainé, P. P.; Ciofini, I.; Ochsenbein, P.; Amouyal, E.; Adamo, C.; Bedioui, F. *Chem.—Eur. J.* **2005**, *11*, 3711. (b) Lainé, P.; Bedioui, F.; Amouyal, E.; Albin, V.; Berruyer−Penaud, F. *Chem.—Eur. J.* **2002**, *8*, 3162. (c) Lainé, P. P.; Bedioui, F.; Loiseau, F.; Chiorboli, C.; Campagna, S. *J. Am. Chem. Soc.* **2006**, *128*, 7510. (d) Lainé, P. P.; Loiseau, F.; Campagna, S.; Ciofini, I.; Adamo, C. *Inorg. Chem.* **2006**, *45*, 5538. (e) Lainé, P. P.; Campagna, S.; Loiseau, F. *Coord. Chem. Rev.* **2008**, *252*, 2552.

(13) Di Pietro, M. L.; Puntoriero, F.; Tuyeras, F.; Ochsenbein, P.; Lainé, P. P.; Campagna, S. *Chem. Commun.* **2010**, *46*, 5169.

(14) Wu, D.; Pisula, W.; Enkelman, V.; Feng, X.; Müllen, K. *J. Am. Chem. Soc.* **2009**, *131*, 9620.

(15) (a) Meyer, T. J. *Pure Appl. Chem.* **1986**, *58*, 1193. (b) Juris, A.; Balzani, V.; Barigelletti, F.; Campagna, S.; Belser, P.; Von Zelewsky, A. *Coord. Chem. Rev.* **1988**, *84*, 85. (c) Sauvage, J. P.; Collin, J. P.; Chambron, J. C.; Guillerez, S.; Coudret, C.; Balzani, V.; Barigelletti, F.; De Cola, L.; Flamigni, L. *Chem. Rev.* **1994**, *94*, 993. (d) Balzani, V.; Juris, A.; Venturi, M.; Campagna, S.; Serroni, S. *Chem. Rev.* **1996**, *96*, 759. (e) Campagna, S.; Puntoriero, F.; Nastasi, F.; Bergamini, G.; Balzani, V. *Top. Curr. Chem.* **2007**, *280*, 117.

(16) Balzani, V.; Scandola, F. *Supramolecular Photochemistry*; Horwood: Chichester, U. K., 1991.

(17) Fortage, J.; Peltier, C.; Perruchot, C.; Takemoto, Y.; Teki, Y.; Bedioui, F.; Marvaud, V.; Dupeyre, G.; Pospisil, L.; Adamo, C.; Hromadova, M.; Ciofini, I.; Lainé, P. P. *J. Am. Chem. Soc.* **2012**, *134*, 2691.

(18) (a) Evans, D. H.; Hu, K. *J. Chem. Soc., Faraday Trans.* **1996**, *92*, 3983. (b) Evans, D. H. *Chem. Rev.* **2008**, *108*, 2113 and references therein.

(19) Puntoriero, F.; Nastasi, F.; Galletta, M.; Campagna, S. In *Comprehensive Inorganic Chemistry II*; Elsevier: Oxford; 2013; Vol. 8, p 255.

(20) Peltier, C.; Lainé, P. P.; Scalmani, G.; Frisch, M. J.; Adamo, C.; Ciofini, I. *J. Mol. Struct.: THEOCHEM* **2009**, *914*, 94.

(21) Kumaresan, D.; Shankar, K.; Vaidya, S.; Schmehl, R. H. *Top. Curr. Chem.* **2007**, *281*, 101 and references therein.

(22) (a) Caspar, J. V.; Meyer, T. J. *J. Am. Chem. Soc.* **1983**, *105*, 5583. (b) Song, W.; Chen, Z.; Brennaman, M. K.; Conception, J. J.; Patrocinio, A. O. T.; Murakami Iha, N. Y.; Meyer, T. J. *Pure Appl. Chem.* **2011**, *83*, 749.

(23) The lowest-energy triplet states of the pyridinium species **A1**−**A5** lie at higher energy than 600 nm (ref 9), so photoinduced energy transfer from ^{3}MLCT states to triplet states centered on the pyridinium units is not a feasible decay process for **1**−**5** compounds.

(24) Gaines, G. L., III; O'Neil, M. P.; Svec, W. A.; Niemczyk, M. P.; Wasielewski, M. R. *J. Am. Chem. Soc.* **1991**, *113*, 719.

(25) Chen, P.; Meyer, T. J. *Chem. Rev.* **1998**, *98*, 1439.

(26) Amouyal, E.; Mouallem-Bahout, M.; Calzaferri, G. *J. Phys. Chem.* **1991**, *95*, 7641.

(27) This first process is evidenced by isolating the transient spectra during the first 10 ps from a laser pulse, see top panel of Figure 6, for **2** as a representative case; the fast kinetic component is connected to a spectral flattening in the 550−650 nm range and to a slight increased absorption for $\lambda > 700$ nm.

(28) (a) Damrauer, N. H.; McCusker, J. K. *J. Phys. Chem. A* **1999**, *103*, 8440. (b) Hammarström, L.; Barigelletti, F.; Flamigni, L.; Indelli, M. T.; Armaroli, N.; Calogero, G.; Guardigli, M.; Sour, A.; Collin, J.-P.; Sauvage, J.-P. *J. Phys. Chem. A* **1997**, *101*, 9061. (c) McCusker, J. K. *Acc. Chem. Res.* **2003**, *36*, 876.

(29) The charge-separated states in **2**−**4** have relatively high energies, so that back electron transfer to the ground state is expected to occur in the Marcus inverted region and can be relatively slow. From an electronic viewpoint, charge recombination towards (and via) the MLCT origin state is the reverse process of that illustrated in Figure 5, involving orbitals that are spatially close to one another, whereas charge recombination to the ground state would involve a metal-centered orbital as the acceptor partner, with a reduced electronic coupling for the process as compared to that associated with the forward electron transfer.

(30) In this case, luminescence lifetime should also be biexponential, with the shorter time related to the equilibration process. However, this cannot be evidenced in our experiments, as the shorter time limit of our apparatus for time-resolved luminescence is 150 ps.

(31) (a) Ford, W. E.; Rodgers, M. A. J. *J. Phys. Chem.* **1992**, *96*, 2917. (b) Tyson, D. S.; Luman, C. R.; Zhou, X.; Castellano, F. N. *Inorg. Chem.* **2001**, *40*, 4063. (c) Wang, X. Y.; Del Guerzo, A.; Schmehl, R. H. *J. Photochem. Photobiol. C: Photochem. Rev.* **2004**, *5*, 55. (d) McClenaghan, N. D.; Maubert, B.; Indelli, M. T.; Campagna, S. *Coord. Chem. Rev.* **2005**, *249*, 1336.

(32) This is namely the CS state for **2** and **4** ($\Delta G_{ET}^{\circ} > 0$) and the MLCT state in the case of **3** ($\Delta G_{ET}^{\circ} < 0$).
(33) Fang, Y.-Q.; Taylor, N. J.; Laverdière, F.; Hanan, G. S.; Loiseau, F.; Nastasi, F.; Campagna, S.; Nierengarten, H.; Leize-Wagner, E.; Van Dorsselaer, A. *Inorg. Chem.* **2007**, *46*, 2854 and references therein.
(34) Burla, M. C.; Caliandro, R.; Camalli, M.; Carrozzini, B.; Cascarano, G. L.; Giacovazzo, C.; Mallamo, M.; Mazzone, A.; Polidori, G.; Spagna, R. *J. Appl. Crystallogr.* **2012**, *45*, 357.
(35) Sheldrick, G. M. *Acta Crystallogr., Sect. A* **2008**, *64*, 112.
(36) Pavlishchuk, V. V.; Addison, A. W. *Inorg. Chim. Acta* **2000**, *298*, 97.
(37) Crosby, G. A.; Demas, J. N. *J. Phys. Chem.* **1971**, *75*, 991.
(38) Nakamaru, N. *Bull. Chem. Soc. Jpn.* **1982**, *55*, 2697.